IEEE Access
Multidisciplinary | Rapid Review | Open Access Journal

SPECIAL SECTION ON MILLIMETER-WAVE AND TERAHERTZ PROPAGATION, CHANNEL MODELING AND APPLICATIONS

Received November 18, 2019, accepted December 24, 2019, date of publication January 8, 2020, date of current version January 15, 2020.

Digital Object Identifier 10.1109/ACCESS.2020.2965003

Millimeter-Wave Communication for a Last-Mile Autonomous Transport Vehicle

ERIK KAMPERT, CHRISTOPH SCHETTLER, ROGER WOODMAN, PAUL A. JENNINGS, AND MATTHEW D. HIGGINS, (Senior Member, IEEE)

WMG, University of Warwick, Coventry CV4 7AL, U.K.

Corresponding author: Erik Kampert (e.kampert@warwick.ac.uk)

This work was supported in part by the Self-organizing Wide-area Autonomous vehicle Real-time Marshaling (SWARM) project, funded by Innovate UK, the U.K.'s Innovation Agency, under Grant 103287, as a collaboration between RDM Group/Aurrigo, University of Warwick and Milton Keynes Council, in part by the WMG Center High Value Manufacturing Catapult, University of Warwick, Coventry, U.K., in part by the Wireless Infrastructure Group, Bellshill, U.K., and in part by the EPSRC through the UK-RAS Network.

ABSTRACT Low-speed autonomous transport of passengers and goods is expected to have a strong, positive impact on the reliability and ease of travelling. Various advanced functions of the involved vehicles rely on the wireless exchange of information with other vehicles and the roadside infrastructure, thereby benefitting from the low latency and high throughput characteristics that 5G technology has to offer. This work presents an investigation of 5G millimeter-wave communication links for a low-speed autonomous vehicle, focusing on the effects of the antenna positions on both the received signal quality and the link performance. It is observed that the excess loss for communication with roadside infrastructure in front of the vehicle is nearly half-power beam width independent, and the increase of the root mean square delay spread plays a minor role in the resulting signal quality, as the absolute times are considerably shorter than the typical duration of 5G New Radio symbols. Near certain threshold levels, a reduction of the received power affects the link performance through an increased error vector magnitude of the received signal, and subsequent decrease of the achieved data throughput.

INDEX TERMS Autonomous vehicles, channel modelling, millimeter-wave propagation, performance evaluation, radio link, vehicular communications.

I. INTRODUCTION

As an enabler of the fifth generation of mobile communication technology, 5G, exploitation of the millimeter-wave (mmWave) spectrum is foreseen to impact various wireless connectivity application areas, including transportation and manufacturing [1]. Both applications will require sub-millisecond latency with error rates lower than one in 10^5 packets dropped, which are enabled by the Ultra-Reliable Low-Latency Communication (URLLC) use case of 5G. Additionally, connected vehicles will benefit from uplink peak data rates of 10 Gb/s that are supported by the massive Machine Type Communications (mMTC) use case [2]. High throughput links could, in particular, facilitate the more advanced functions and capabilities of self-driving vehicles. For example, see-through and non-line-of-sight (NLOS) sensing, for which raw vehicular sensor data or videos potentially need to be shared between vehicles and with the roadside infrastructure [3].

The first self-driving vehicles that will be deployed on public and private roads are expected to be low-speed autonomous pods, dedicated to last-mile transportation of goods and passengers. The SWARM project aims to develop a fleet of level 4 low-speed, autonomous pods (Aurrigo SWARM pods), which can coalesce and travel as platoons, as illustrated in Figure 1 [4]. The pods are typical future vehicles for last-mile transport, which can be used on public pavements, streets, and on private land. They are anticipated to complement existing transport modalities, providing new, more bespoke options for travel. This will be particularly important for those that are unable to use other forms of transportation, such as people with mobility issues, the elderly, and young children [5]. Pods use vehicle-to-vehicle (V2V) communication to plan their route in order to maximize platooning opportunities. In addition to local communication, pods will need to maintain a connection to the operations

The associate editor coordinating the review of this manuscript and approving it for publication was Ke Guan.

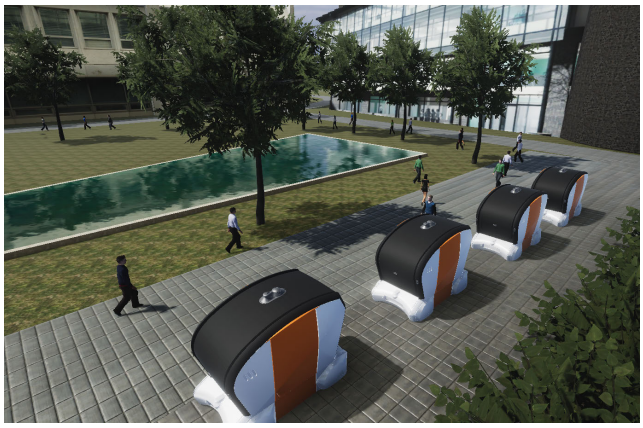

FIGURE 1. Virtual representation of platooning Aurrigo SWARM pods on the University of Warwick campus benefitting from 5G mmWave V2I communication.

center, from where supervisors will track their movement via real-time, high definition (HD) video. If there is a drop in the connection, or a delay over 100 ms, the pod will automatically stop. Therefore, the pod system requires both a high throughput to carry such video, and an uninterrupted connection to ensure a smooth journey for passengers. Early 2020, these pods will be deployed on various routes on the campus of the University of Warwick, as part of its Connected Autonomous Vehicles (CAV) Testbed [6]. Among others, in this role, they will also be used for the first capability demonstrations and studies of 5G connectivity, initially focusing on high data throughput from infrastructure to pod passengers, e.g. non-critical delivery of HD video entertainment.

The aim of the research described in this paper, is to understand the implications of antenna placement for vehicle-to-infrastructure (V2I) communications, particularly focusing on low-speed autonomous pods. Hence, the positions of transmitting antennas (TX) and receiving antennas (RX) are varied around and inside the Aurrigo SWARM pod. The crucial output parameters of interest are the measured excess loss (EL) and the root mean square delay spread (RMS-DS), which can be directly determined from the obtained measurement results. EL provides a direct measure of the lost signal power due to reflection, absorption, and refraction from objects and materials that are in the communication path from TX to RX. RMS-DS weighs reflected signals based on their power and distance to the line-of-sight signal (LOS), and therefore is a measure of the multipath component (MPC) richness of the observed signals. MPCs lead to interference, with a typical rule of thumb that intersymbol interference (ISI) is likely to occur for signals that are shorter than ten times the RMS-DS value.

A second aim of the research is to understand how the typical signal quality parameters of a vehicular communication channel depend on its environment. Of particular interest are the error vector magnitude (EVM) and the achieved data throughput, which provide information on the channel's usability for specific information transfer. Moreover, such parameters can then be directly related to the determined EL and RMS-DS values, in order to observe general trends and dependencies. Optimal vehicular and roadside infrastructure antenna locations can be determined from the reported quality of signal parameters.

II. BACKGROUND

The last decade has seen a particular increase of industrial and academic interest in mmWave communications. Numerous indoor and outdoor measurement campaigns have been carried out, with the joint goal to understand mmWave propagation characteristics and to mathematically describe them in a channel model. As the observed small and large-scale fading behavior is strongly environment-dependent, channel models have been developed for groups of scenarios and comprehensively summarized in individual papers and surveys [7], [8]. As one of the most promising initial applications, mmWave vehicular communications received considerable attention, with a variety of measurements and modelling carried out, ranging from understanding the impact of vehicular velocity through a Doppler shift of the mmWave signal, to understanding in detail the influence of precipitation on mmWave attenuation [9], [10]. In turn, these experimental observations and subsequent parameterization have equipped others with path loss exponents to develop half-power beam width (HPBW) dependent vehicular sensor data broadcasting schemes and vehicle distribution dependent coverage models [11], [12].

With the 3rd Generation Partnership Project's (3GPP) Release 15 of the New Radio (NR) mobile telecommunication standard matured and completed, the collaboration of standard development organizations aims to finish an initial full 5G system by mid-2020 through completion of Release 16. This release will cover specific work for vehicle-to-everything (V2X) application layer services and includes study items to target advanced V2X use cases, such as extended sensing and remote driving. Continuing enhancements and optimization of, among others, edge computing and network security in Release 17 are foreseen to benefit the vehicular communication domain in the future [13].

III. EXPERIMENTAL DETAILS

The goal of the following mmWave channel investigation is to evaluate the possibilities to establish a reliable V2I communication link with the Aurrigo SWARM pod, and understand both the impact of its structure on the received radio frequency (RF) signal, as well as the consequences for the link performance. From an RF point-of-view, such a pod has a much simpler construction than a more traditional car; in the absence of crumple zones and a motor block, the vehicle mainly consists of a metallic frame that supports metal doors at its sides. The pod is located inside the WMG 3xD Simulator at the University of Warwick [14]. The 3xD Simulator is housed inside a Faraday cage, and absorbing material on the walls and roof makes the room anechoic for radio frequency radiation with frequencies above 1.3 GHz. A mobile board,

fitted with absorbing material, provides blockage of signal reflections from the experimental setup itself.

For this particular study, the focus lies on a carrier frequency of 28.5 GHz, as a representative of the prioritized first high frequency band for 5G in Europe. In order to understand the impact of the SWARM pod's structure on 5G signals received inside it, an ultra-wideband omnidirectional RX with a typical gain of 6 dBi and an elevation HPBW of 20° is placed at the center of the front headrest. Besides representing a 5G user sitting at the front end of the pod, this antenna location could also be used for information that the pod needs to share with other vehicles or roadside infrastructure. TX is positioned at a horizontal distance of 2.6 m from RX, at various heights and azimuthal angles to represent the locations at which such infrastructure might be placed, and is boresight aligned with RX. Figure 2 displays the RX location inside the pod, and, clockwise, the gradually changing boresight view of TX, for three different antenna heights, namely at equal height with RX at 1.4m; at the lower end of a traffic signal assembly at 2.1 m; and at the red light of a traffic signal assembly at 3.0 m. For the latter height, measurements are performed for both aligned and unaligned RX, in order to understand the impact of its antenna pattern. At each position, measurements are performed consecutively with three directional waveguide horn antennas, varying the HPBW from 10° to 30° to 55°. The different antenna gains of each waveguide are taken into account in the analysis of the measurement results.

Our channel sounding equipment uses the pulse compression method and consists of an R&S SMW200A vector signal generator, an R&S SMZ90 frequency multiplier, an R&S FSW85 signal and spectrum analyzer and an R&S RTO2044 digital oscilloscope. Further details on the facility and our channel sounding methodology can be found in our previous work [15].

The subsequent link performance experiments are carried out using the NI mmWave Transceiver System (MTS), with similar hardware components that others have also reported for mmWave channel sounding measurements [16]–[18]. The MTS is a software-defined radio with 2 GHz of real-time bandwidth that can be used to create over-the-air prototypes of 5G NR communications links. A multi-FPGA processing architecture enables to both capture and generate 2 GHz of data and to process it in real time. The MTS is a modular system and built from a common set of PXI Express hardware: a PXIe-3610 digital-to-analog converter (DAC), a PXIe-3630 analog-to-digital converter (ADC), and a PXIe-3620 local oscillator and intermediate frequency module. Each DAC and ADC is paired with a PXIe-7902 FPGA module for (de)modulation. A PXIe-6674T timing and synchronization module provides a high quality 10 MHz clock source and a trigger for synchronization of multiple channels. Outside of the PXI chassis, the MTS is connected to mmWave heads: a mmRH-3642 transmitter and a mmRH-3652 receiver, optimized for the frequency band from 27.5 to 29.5 GHz, with 2 GHz instantaneous bandwidth and an analog gain range

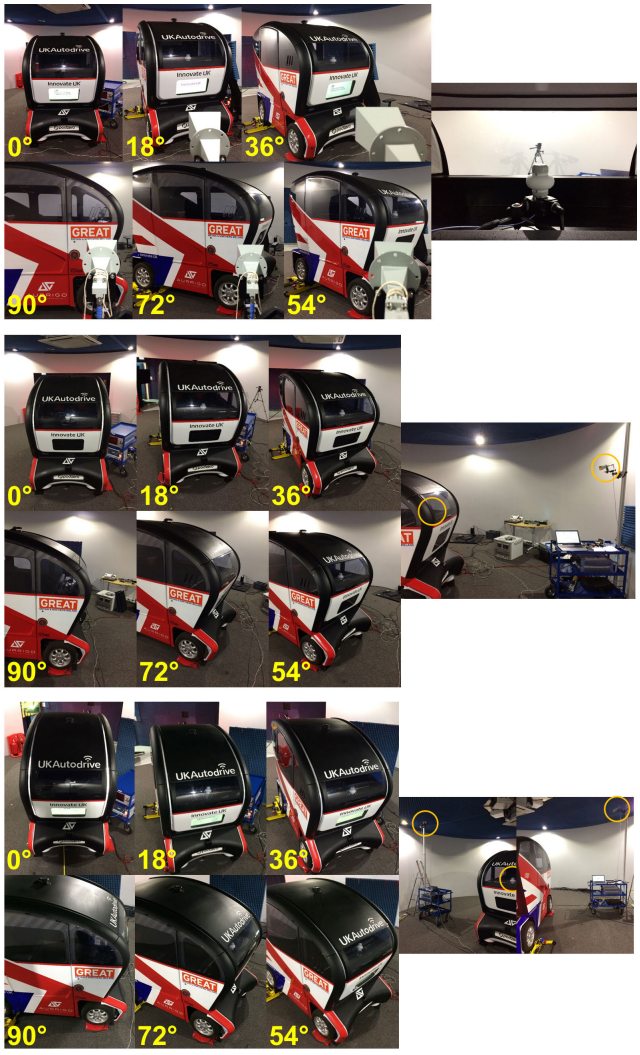

FIGURE 2. Photos of the V2I channel measurements with the RX location inside the pod (antennas encircled), and the corresponding TX location (boresight view, azimuth in yellow) at 1.4 m height (top), 2.1 m height (middle) and 3.0 m height (bottom).

of at least 50 dB. In addition to the RF hardware in the MTS, four additional FPGAs are added to the system to create a real-time 5G NR physical layer and to allow for real-time encoding and decoding of the communication link's signal, which enables a data throughput calculation. For the measurements and results presented herein, the MTS software configuration follows the Verizon 5G specifications, using eight 100 MHz component carriers resulting in a total 800 MHz bandwidth, a cyclic prefix orthogonal frequency-division multiplexing (CP-OFDM) waveform, dynamic time-division duplexing (TDD), turbo coding, and as possible modulation schemes quadrature phase shift keying (QPSK), 16-QAM and 64-QAM (quadrature amplitude modulation).

IV. CHANNEL SOUNDING RESULTS AND DISCUSSION

For an appropriate and clear comparison with other channel sounding reports, the EL and RMS-DS parameters are

extracted from the channel sounder's calculated power delay profiles (PDP). EL is defined as the difference between the received power level and the expected power level, based on a free-space path loss model, and taking into account signal losses and gains due to the used equipment, based on extensive calibration measurements. The RMS-DS is the common, standard deviation of the delay times τ between the LOS and a significant MPC, which are weighted by the received power at that time, PDP(τ), according to

$$\text{RMS} - \text{DS} = \sqrt{\frac{\int (\tau - \tau_m)^2 \cdot \text{PDP}(\tau)\, d\tau}{\int \text{PDP}(\tau)\, d\tau}},$$
$$\tau_m = \frac{\int \tau \cdot \text{PDP}(\tau)\, \text{d}\tau}{\int \text{PDP}(\tau)\, \text{d}\tau} \quad (1)$$

Figure 3 displays the measured EL and RMS-DS for the various antenna constellations and different HPBW. Upon increasing the TX height from 1.4 to 3.0 m, EL and RMS-DS increase for all HPBW by either reducing or obscuring the field of view of TX's beam and thereby its overlap with RX. Moreover, due to the time resolution of the experimental setup, MPCs with lengths within 30 cm of the LOS-path are included in the measured LOS-signal and not distinguished as individual MPCs. Hence, with increasing TX height, the increased distance in the tilted TX-RX plane to the nearby pod frame and doors might reduce the possible number of MPCs very close to the LOS-signal, resulting in a higher EL and RMS-DS.

When TX is at a height of 3.0 m and RX is additionally boresight aligned with TX, EL decreases with 5 to 10 dB, in accordance with the RX antenna pattern. Since the used TX-RX distances and angles are based on realistic traffic settings, this displays that in order to optimize mmWave connectivity for this use case, either a beam steerable antenna or a wide beam horn antenna should be implemented at the vehicle's end. For the lowest and highest TX height and all HPBW, EL increases with 6 to 10 dB at an azimuth of 72°, when the TX field of view is largely obscured by the curved metal frame of the SWARM pod's front window.

EL is nearly HPBW-independent as the LOS-path is unchanged, except for the time resolution reasons mentioned previously. However, DS does depend on the HPBW, as a wider TX antenna beam generates more and longer MPCs inside the pod. To put this into perspective, at a distance of 3.0 m an antenna beam of 10°, 30° and 55° is 0.5 m, 1.6 m and 3.1 m wide. Hence, DS increases with HPBW until the TX antenna beam covers the complete pod, more than doubling the measured DS from 2 to 5 ns.

V. LINK PERFORMANCE RESULTS AND DISCUSSION

Link performance measurements on the SWARM pod are carried out for a selection of antenna constellations, which have been used in the previous channel sounding section of this paper. Besides providing an understanding of the achievable data throughput and EVM for such V2I scenario, this also allows for a direct comparison with the previous results

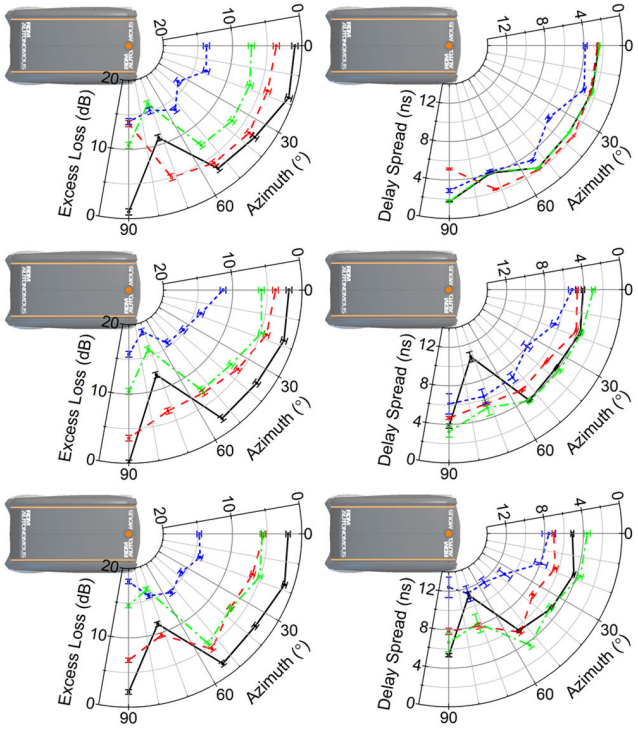

FIGURE 3. Left column: HPBW-dependent polar plots of the measured EL in the V2I channel from roadside infrastructure at various heights (see Fig. 1) to the center of the pod's front headrest at a height of 1.4 m (the plot's origin). For a carrier frequency of 28.5 GHz, the EL is plotted versus the antenna pair orientation with the error bars indicating one standard deviation interval. Waveguide horn antennas with a typical gain/HPBW of 25 dBi / 10° (top); 15 dBi / 30° (middle); and 10 dBi / 55° (bottom) are used as TX. The lines connecting the measured values are guides to the eye (black solid = 1.4 m; red dashed = 2.1 m, green dash dotted = 3.0 m; blue short dashed = 3.0 m with unaligned RX). Right column: HPBW-dependent polar plots of the measured RMS-DS versus antenna pair direction in the V2I channel from roadside infrastructure at various heights to the center of the pod's front headrest.

from the channel sounding measurements. The EVM is a measure of the difference between the reference waveform and the measured waveform, and can be linked to the signal-to-noise ratio (SNR) and bit error rate (BER) [19]. As the aim is to achieve maximum possible data throughput, a 64-QAM scheme with a 7/8 code rate is chosen, resulting in a maximum throughput of 2.867 Gb/s.

Figure 4 displays the measured EVM and data throughput for various antenna constellations and different HPBW; with TX boresight aligned with RX, and RX additionally boresight aligned with TX at a height of 3.0 m. Increasing the TX height increases the EVM and reduces the data throughput for all HPBW by reducing/obscuring the field of view of TX's beam. For few antenna constellations, the LOS path is unobscured, and a maximum data throughput of 2.867 Gb/s is achieved. For other heights, the quality of the communication path is so poor, that the data throughput is almost fully stopped and the EVM is accordingly high. With increasing HPBW, the output power of the MTS transmitter is increased to the maximum of 27 dBm in order to achieve a detectable throughput for any antenna constellation. Nevertheless, maximum achievable throughput is reduced to 1.1 Gb/s and 0.5 Gb/s for the 30°

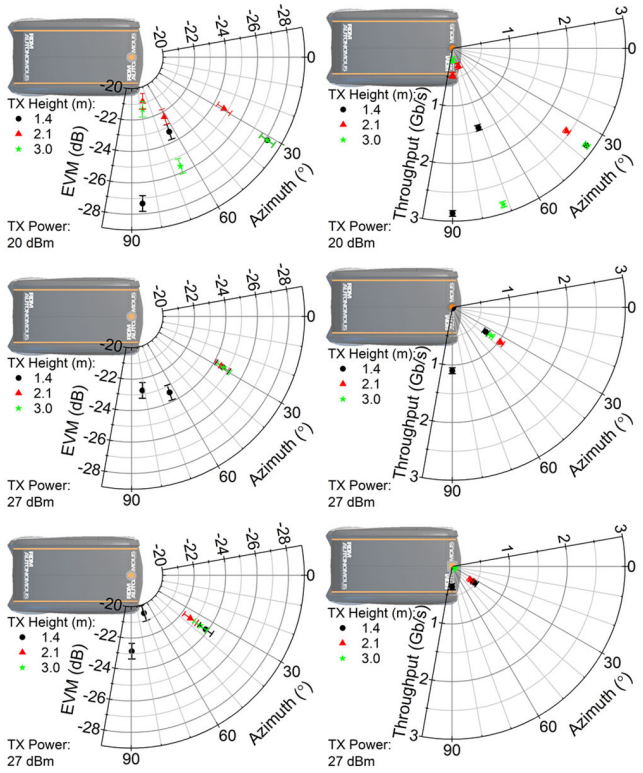

FIGURE 4. Left column: HPBW-dependent polar plots of the measured EVM in the V2I channel from roadside infrastructure at various heights (see Fig. 1) to the center of the pod's front headrest at a height of 1.4 m (the plot's origin). For a carrier frequency of 28.5 GHz and a 64-QAM scheme with a 7/8 code rate, the EVM is plotted versus the antenna pair orientation with the error bars indicating one standard deviation interval. Waveguide horn antennas with a typical gain/HPBW of 25 dBi / 10° (top); 15 dBi / 30° (middle); and 10 dBi / 55° (bottom) are used as TX (output power at bottom left). Right column: HPBW-dependent polar plots of the measured data throughput versus antenna pair direction in the V2I channel from roadside infrastructure at various heights to the center of the pod's front headrest.

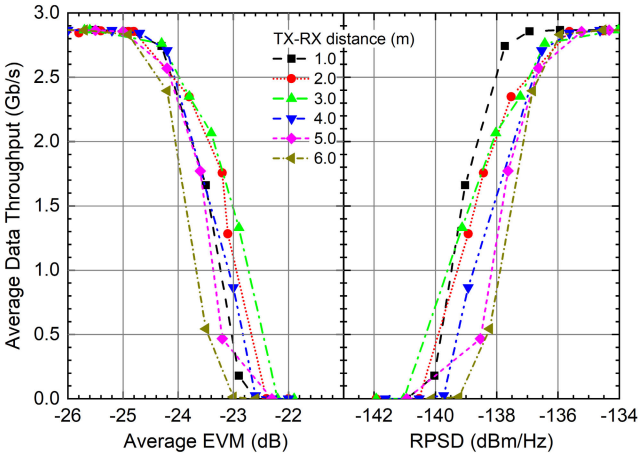

FIGURE 5. Left: Measured averaged data throughput in a line of sight communication link between a 10° HPBW waveguide horn antenna and an ultra-wideband omnidirectional antenna for various antenna separations (see legend). For a carrier frequency of 28.5 GHz and a 64-QAM scheme with a 7/8 code rate, the throughput is plotted versus the measured averaged EVM. Right: Data throughput versus the received power spectral density, which values are based on channel sounding measurements, for various antenna separations.

and 55° HPBW antenna, respectively, with EVM increasing accordingly.

In order to allow for a detailed comparison between the channel sounding and link performance results, additional systematic measurements are carried out, involving the same, boresight aligned 10° HPBW TX horn antenna and omni-directional RX at fixed antenna distances in a clear LOS set-up inside the WMG 3xD Simulator. For various TX-RX distances, the TX output power is stepwise reduced, and the resulting EVM and throughput are compared with precise RX received power values from channel sounding measurements. Due to the bandwidth difference between both methods, 800 MHz versus 2 GHz, the received power is divided by the used bandwidth in order to obtain the Received Power Spectral Density (RPSD).

Figure 5 displays the measured averaged data throughput versus EVM and RPSD for increasing TX-RX antenna separation. The plots show a clear threshold behavior below which the throughput approaches its maximum and above which the throughput is reduced to zero. These thresholds are almost TX-RX separation independent, hence are 5G NR specific. The plots indicate, that for full throughput in a 64-QAM scheme, the minimum required EVM is −25 dB and the minimal required RPSD to achieve this is −135 dBm/Hz. Additional measurements for the 16-QAM (7/8 code rate) and QPSK (3/4 code rate) modulation schemes yield a −18 dB EVM and −142 dBm/Hz RPSD threshold for a maximum 16-QAM throughput of 2.0 Gb/s; and −10 dB and −148 dBm/Hz thresholds for a maximum QPSK throughput of 0.8 Gb/s, respectively. Further, preliminary results also show that these dependences are HPBW-independent.

Because the modulation scheme determines the maximum possible data throughput, these results can be used to optimize the data throughput in a given scenario by switching between modulation schemes. For instance, the 64-QAM scheme should be used for data throughputs larger than 2 Gb/s and signals with an RPSD larger than −137 dBm/Hz; for an RPSD between −137 dBm/Hz and −144 dBm/Hz the 16-QAM scheme delivers throughputs larger than 0.8 Gb/s; and for an RPSD smaller than −144 dBm/Hz the QPSK modulation scheme still delivers data following the steepness of its threshold.

VI. CONCLUSION

The experimental results presented in this paper show the possibility to create a high quality 5G mmWave communication link with a low-speed autonomous vehicle in a typical V2I scenario. For various antenna constellations, it is shown that the experienced EL is almost HPBW-independent, whereas the received power decreases. Although DS increases with HPBW, the main impact on the link performance is through the reduced RX power, with a threshold behavior of both EVM and data throughput for an RPSD below −135 dBm/Hz

when a 64-QAM scheme is used. Knowledge about such thresholds for all modulation schemes can be exploited, among others, by a vehicular communication system that uses the RPSD to select the scheme with highest link performance under those circumstances, in order to provide an optimal, reliable V2I communication link.

REFERENCES

[1] A. Ghosh, T. A. Thomas, M. C. Cudak, R. Ratasuk, P. Moorut, F. W. Vook, T. S. Rappaport, G. R. Maccartney, S. Sun, and S. Nie, "Millimeter-wave enhanced local area systems: A high-data-rate approach for future wireless networks," *IEEE J. Sel. Areas Commun.*, vol. 32, no. 6, pp. 1152–1163, Jun. 2014.

[2] *Minimum Requirements Related to Technical Performance for IMT-2020 Radio Interface(s)*, document ITU-R M.2410-0, International Telecommunication Union, Geneva, Switzerland, Nov. 2017. Accessed: Oct. 31, 2019. [Online]. Available: https://www.itu.int/dms_pub/itu-r/oth/0c/0a/R0C0A00000C0014PDFE.pdf

[3] *Technical Specification Group Services and System Aspects. Enhancement of 3GPP Support for V2X Scenarios*, document 3GPP TS 22.186 V16.2.0, 3rd Generation Partnership Project, Valbonne, France, Jun. 2019.

[4] R. Woodman, K. Lu, M. D. Higgins, S. Brewerton, P. A. Jennings, and S. Birrell, "Gap acceptance study of pedestrians crossing between platooning autonomous vehicles in a virtual environment," *Transp. Res. F, Traffic Psychol. Behav.*, vol. 67, pp. 1–14, Nov. 2019.

[5] S. Pettigrew, S. L. Cronin, and R. Norman, "Brief report: The unrealized potential of autonomous vehicles for an aging population," *J. Aging Social Policy*, vol. 31, no. 5, pp. 486–496, Oct. 2019.

[6] Accessed: Oct. 31, 2019. [Online]. Available: https://midlandsfuture mobility.co.uk

[7] S. Sun, T. S. Rappaport, T. A. Thomas, A. Ghosh, H. C. Nguyen, I. Z. Kovacs, I. Rodriguez, O. Koymen, and A. Partyka, "Investigation of prediction accuracy, sensitivity, and parameter stability of large-scale propagation path loss models for 5G wireless communications," *IEEE Trans. Veh. Technol.*, vol. 65, no. 5, pp. 2843–2860, May 2016.

[8] I. A. Hemadeh, K. Satyanarayana, M. El-Hajjar, and L. Hanzo, "Millimeter-wave communications: Physical channel models, design considerations, antenna constructions, and link-budget," *IEEE Commun. Surveys Tuts.*, vol. 20, no. 2, pp. 870–913, 2nd Quart., 2018.

[9] V. Va, J. Choi, and R. W. Heath, "The impact of beamwidth on temporal channel variation in vehicular channels and its implications," *IEEE Trans. Veh. Technol.*, vol. 66, no. 6, pp. 5014–5029, Jun. 2017.

[10] C. Han and S. Duan, "Impact of atmospheric parameters on the propagated signal power of millimeter-wave bands based on real measurement data," *IEEE Access*, vol. 7, pp. 113626–113641, 2019.

[11] X. Chen, S. Leng, Z. Tang, K. Xiong, and G. Qiao, "A millimeter wave-based sensor data broadcasting scheme for vehicular communications," *IEEE Access*, vol. 7, pp. 149387–149397, 2019.

[12] M. Ozpolat, E. Kampert, P. A. Jennings, and M. D. Higgins, "A grid-based coverage analysis of urban mmWave vehicular ad hoc networks," *IEEE Commun. Lett.*, vol. 22, no. 8, pp. 1692–1695, Aug. 2018.

[13] A. Ghosh, A. Maeder, M. Baker, and D. Chandramouli, "5G evolution: A view on 5G cellular technology beyond 3GPP release 15," *IEEE Access*, vol. 7, pp. 127639–127651, 2019.

[14] S. Khastgir, S. Birrell, G. Dhadyalla, and P. Jennings, "Identifying a gap in existing validation methodologies for intelligent automotive systems: Introducing the 3xD simulator," in *Proc. IEEE Intell. Vehicles Symp. (IV)*, Jun. 2015, pp. 648–653.

[15] E. Kampert, P. A. Jennings, and M. D. Higgins, "Investigating the V2V millimeter-wave channel near a vehicular headlight in an engine bay," *IEEE Commun. Lett.*, vol. 22, no. 7, pp. 1506–1509, Jul. 2018.

[16] Y. J. Cho, G.-Y. Suk, B. Kim, D. K. Kim, and C.-B. Chae, "RF lens-embedded antenna array for mmWave MIMO: Design and performance," *IEEE Commun. Mag.*, vol. 56, no. 7, pp. 42–48, Jul. 2018.

[17] T. S. Rappaport, G. R. Maccartney, M. K. Samimi, and S. Sun, "Wideband millimeter-wave propagation measurements and channel models for future wireless communication system design," *IEEE Trans. Commun.*, vol. 63, no. 9, pp. 3029–3056, Sep. 2015.

[18] G. R. Maccartney and T. S. Rappaport, "A flexible millimeter-wave channel sounder with absolute timing," *IEEE J. Select. Areas Commun.*, vol. 35, no. 6, pp. 1402–1418, Jun. 2017.

[19] R. Shafik, M. Rahman, A. Islam, and N. Ashraf, "On the error vector magnitude as a performance metric and comparative analysis," in *Proc. Int. Conf. Emerg. Technol.*, 2006, pp. 27–31.

ERIK KAMPERT received the M.Sc. and Ph.D. degrees in natural sciences from the Radboud University Nijmegen, The Netherlands, in 2005 and 2012, respectively. He was with the Molecular Materials Group and the High Field Magnet Laboratory within the Institute for Molecules and Materials, RU. He continued his research as a Postdoctoral Researcher with the Dresden High Magnetic Field Laboratory, Helmholtz-Zentrum Dresden-Rossendorf, Germany, where he conducted electrical transport experiments in pulsed magnetic fields in collaboration with visiting, international scientists. In 2017, he joined the Connectivity Group within WMG's Intelligent Vehicles Research Team, University of Warwick, U.K., as a Senior Research Fellow. Using his vast background in RF electromagnetics, the focuses of his current research are on 5G millimeter-wave communication for vehicular-to-everything, and industrial Internet of Things applications.

CHRISTOPH SCHETTLER is currently pursuing the combined B.Sc. and M.Phys. degrees in physics with the University of Warwick, U.K. He is completing the Master of Physics on bacterial chemotaxis under antibiotic challenge in a collaborative effort between the Department of Physics and the School of Life Sciences at the University of Warwick. In 2018, he was a Warwick Research Intern with WMG's Intelligent Vehicles Research Team focusing on experimental research of 5G millimeter-wave communication technologies for connected and autonomous vehicles. His further research interests include the applications of artificial intelligence and data science.

ROGER WOODMAN received the B.Sc. degree in computer science from the University of Gloucestershire, in 2006, the M.Sc. degree in robotics from the University of the West of England, in 2008, and the Ph.D. degree from the Bristol Robotics Laboratory, in 2013. He has over six years of industrial experience, working in leading manufacturing, defence, and software companies. He joined the University of Southampton, in 2013, as a Research Fellow, specializing in biomedical imaging. In 2017, he joined WMG, University of Warwick, as a Research Fellow, where he investigates human factors aspects of low-carbon autonomous transport. He has several scientific articles published in the field of autonomous vehicles and robotics and lectures in the field of autonomous vehicle safety. He is also an Associate Fellow of the HEA.

PAUL A. JENNINGS received the B.A. degree in physics from the University of Oxford, in 1985, and the Engineering Doctorate degree from the University of Warwick, Coventry, in 1996. From 1985 to 1988, he was a Physicist with Rank Taylor Hobson. Since 1988, he has been working on industry-focused research with WMG, University of Warwick. He is currently WMG's Research Director and Lead of the multidisciplinary Intelligent Vehicles Research Team. His current interests include complex electrical systems, communications, experiential engineering, cyber security, modeling and simulation, visualization, and business and operations for automotive and healthcare applications.

MATTHEW D. HIGGINS (Senior Member, IEEE) received the M.Eng. degree in electronic and communications engineering and the Ph.D. degree in engineering from the School of Engineering, University of Warwick, in 2005 and 2009, respectively. After then, he progressed through several Research Fellow positions, in association with some of the U.K.'s leading defence and telecommunications companies before undertaking two years as a Senior Teaching Fellow in telecommunications, electrical engineering and computer science subjects. In July 2012, he was promoted to the position of Assistant Professor, where his research focused on optical, nano, and molecular communications, while in this position, he set up the Vehicular Communications Research Laboratory which aimed to enhance the use of communications systems within the vehicular space. In March 2016, he was promoted, and appointed as an Associate Professor with WMG working in the area of Connected and Autonomous Vehicles, where he leads the ICT and 5G themes of the group. He is also a FHEA, and a member of the EPSRC CommNet2 and the EPSRC Peer Review College.